Knee Cartilage Segmentation using Geodesic Active Contours

Gourab Ghosh Roy*, Mohammed Rami Koujan** and Raabid Hussain***
VIBOT, Escola Politcnica Superior
Universitat de Girona
c/ Maria Aurlia Capmany, 61, 17071, Gerona, Spain
myself.gourab@gmail.com, mhd.kou@gmail.com, raabid236@gmail.com

***Abstract*— This paper presents a geodesic active contour based segmentation technique for femur and tibia components in the magnetic resonance images (MRI) of knee. Intensity and local variance based Geodesic snake structures are used to extract the bone features form the image. Initial seeds are placed within the bone area on selected image slices. The propagation of seeds is performed slice by slice to obtain the final shape of the bone. The femoral and tibial cartilages are extracted using region growing on correlation image of the scan. The algorithm was tested on SKI 10 dataset, the results of which are also discussed.**

I. INTRODUCTION

Knee is one of the largest and most delicate joints in the human body. It consists of four main bones: femur, tibia, patella and fibula. The knee joint consists of soft tissues like ligaments for improving strength and cartilages for lubrication during motion. However over time, the knee structures specially the cartilages start to wear causing painful diseases like osteoarthritis [1]. Surgeons have classified the risk of encountering knee problems equivalent to the risk of having a cardiac disease.

In order to detect structural changes in the knee, modern day non-invasive medical imaging techniques are being exploited. MRI has proved to be the most promising one as it provides direct high spatial images of the entire knee joint, in particular the cartilages [2]. 3D models of the knee created from these images can help simulate the behavior of the knee leading to better diagnosis and treatment [3][4].

Many different approaches have been proposed to segment the structures in the knee. Since the information in the MRI images has low signal to noise ratio, resolution and contrast [5][6], this particular segmentation problem has not yet yielded a satisfactory solution. This mainly arises due to the fact that there are no distinct separations between different structures in the images.

Thus far, clinical applications of knee segmentation have mainly been accomplished either manually [7][8] or semi-automatically. Earlier works in segmentation of medical images include techniques based on region growing, thresholding and edge based algorithms [5]. However, due to the low contrast quality of medical images, these methods were found to be insufficient yielding in spread and overlap of different anatomical structures [3]. Most of the later works include the results of these basic segmentation techniques as an initial result and attempt to build on from them [9][10].

Semi-automatic methods mostly start by interpreting user defined scribbles as shape, position and/or image intensity priors. [11] and [12] use graph based methods, [13] uses watershed models, [14] uses active shape models and [15] uses k-nearest neighbor technique to segment the knee structures. Deformable geometric models and level sets have also been utilized in [4][16][17]. These methods use curve evolution theory to realize the geometric changes. Slight modifications of these techniques are able to define objects whose boundaries are not prominent in gradient images [18].

Although a completely automatic stand alone scheme seems distant, many attempts have been made as in [11][19] to try to make the segmentation as automatic as possible. These methods rely on atlas based techniques. Different qualities of the segmentation regions are learned from previous segmentation results attained through the help of an expert [20][21][22][23]. Registration frameworks are then used to map the atlas structures on to the image under study [24].

This paper focuses on implementation of a knee segmentation technique primarily based on the approach in [19]. The femur and tibia bones are segmented using geodesic active contour snake-like structures whereas their respective cartilages are segmented using region growing. Region growing uses local properties of regions whereas active shape models only use the boundary statistics in order to minimize some energy function. Active shape models have become popular in medical imaging as they can capture the complex or irregular structures [25] found in human structures. There have been many other works that have combined these two strategies such as in [26] and [27]. The human input in our proposed algorithm has been kept to a minimum: 3 seed points per bone type and 2-4 seed points for cartilages. All other parameters have been tuned to their respective optimum values. For implementation, ITK and Mevislab softwares were used.

The rest of the paper is organized as follows: First a general overview of the segmentation scheme is proposed. The different components used in bone and cartilage segmentations are explained next. The paper concludes after detailed analysis of the segmentation results and final remarks.

II. METHODOLOGY

MRI is associated as the best modality for knee joint imaging as it does not use any ionizing radiations and can provide relatively distinct spatial information of the

entire knee structure. A sample MRI image of the knee and different segmented regions are shown in Fig. 1. The bones are clearly visible in a dark gray color whereas the fat structures surrounding the bones are in relatively lighter shades. However, as can be seen near the top of the femur bone that the bone region and its neighboring structures have very less difference in intensity values. Also, although in some of the slices the bone sections are clearly separated from the background regions but in some slices since the difference in intensity values is very less so techniques like region growing and thresholding yield unsatisfactory results. This specially is caused due to the fact that the images are in 3D and even if in one slice the regions are clearly distinct, they might be connected through adjacent slices. A sample output of the region growing algorithm is shown in Fig. 2.

In order to negate the effects of the above-mentioned problems, a segmentation technique based on geodesic active contours for bone and region growing for cartilage is proposed in this paper. The bone and cartilage regions are treated separately. For the bone, seeds are placed at chosen locations on some of the slices to generate level sets. An edge image is also produced from the original image. Both these are input to the geodesic active contours algorithm to yield the segmentation result that is later thresholded to get the final image of the bones. The flow diagram of this process is shown in Fig. 3. For the cartilages, a correlation texture image is produced to make the cartilage regions distinct and visible. The cartilages are then extracted using region growing algorithm. The bone and cartilage regions are then combined after some post-processing to produce the final output.

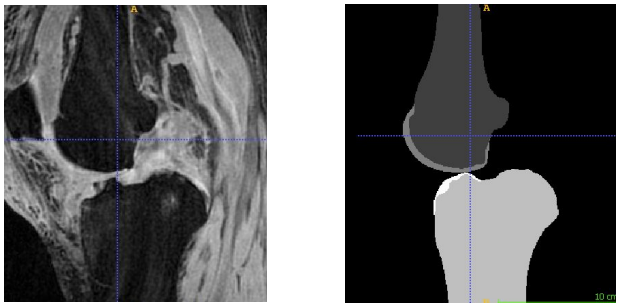

Fig. 1: Sample MRI scan of the knee joint along with its ground truth. The white region in ground truth image represents the tibial cartilage, light gray represents the tibial bone, gray represents the femur cartilage and dark gray represents the femur bone (taken from the SKI 10 dataset).

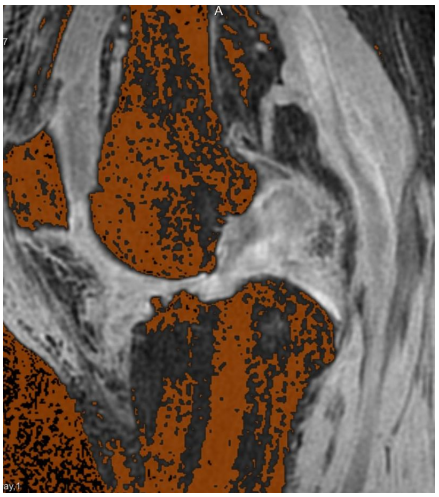

Fig. 2: Sample output of the region growing algorithm. The brown color represents the output for the femur bone.

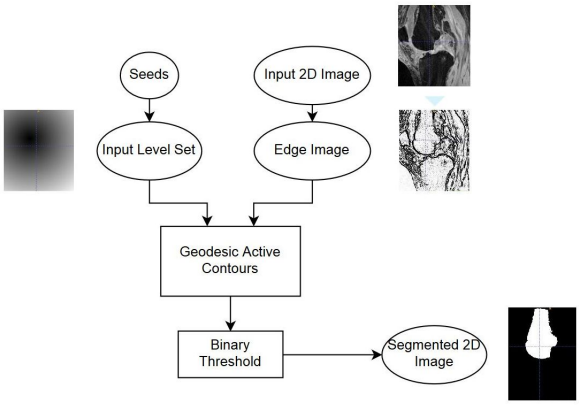

Fig. 3: Flow-diagram of the segmentation algorithm for the bone regions.

III. Bone Segmentation

For segmenting the bone structures from the original images geodesic active contours were used. The geodesic contour block in ITK takes two inputs: input level sets and a gradient image.

A. Input Level Sets

The algorithm starts by asking the user to input the location of the centers for each initial level set. Ideally, the seeds should be placed separately on all slices. The ideal estimate of the input level set is to draw the contours near (inner side) the actual edges of the boundaries of the region of interest as shown in Fig. 4. This leads to a more accurate result with a faster convergence. However, this demands a lot of user input, making the algorithm tedious and time consuming (for drawing the level sets on each slice separately).

So in order to limit the user input, user is asked to select 3 points for each bone type in the entire volume. This is based on the idea that the entire volume can be divided into 5 main parts as shown in Fig. 5. In the starting and ending slices (Fig. 5a, 5e), there is no bone so no seeds need to be placed on them. As we move towards the center of the volume the bone starts appearing and a seed is placed on Fig. 5b, 5d in the middle of the bone area. For improving the quality of the output, a different central seed location is chosen for the slices in the center (5c) because the bones have a different anatomical structure in these slices.

Since we need a geometrical shape as the input level set but we only take the middle point of the bone as seed, a

Fig. 4: Ideal contour to be used as input seeds.

small circle as shown in Fig 6a is drawn over the selected seed points. The radius of this circle is chosen based on the section the slice belongs to, as discussed before. In practice we use a 'fast marching' filter to create an input level set over the entire volume. The fast marching filter computes a distance function by sweeping through all the pixels in the slice. In this implementation, we keep all the points on the circle to be 0, all the points inside the circle to be negative and all the points outside the circle as positive. A sample level set as the output of the fast marching filter is shown in Fig. 6b .

B. Gradient Image

For the Gradient image, a series of pre-processing steps are applied. When the MRI images are being generated, different types of noises are also acquired. Although this noise can not be perfectly classified as a single type of noise but it mainly follows rician distribution. This is the reason that the bones are not of uniform intensities. To remove this noise and smooth out the image, anisotropic diffusion was used. Anisotropic diffusion can be characterized as a non-linear and space-variant transformation of the image itself. It generates a set of images with the different degree of diffusion/smoothing and then removes the noise by combining all the generated images. The main reason for using this filter is that it preserves edges while smoothing out the uniform areas.

After getting the de-noised volume, a gradient extraction filter is applied to obtain a gradient image. The gradient images are passed through a sigmoid filter before inputting into the geodesic active contours function. The sigmoid filter transforms the intensity values of the gradient image smoothly to a specified range. Sigmoid filters are commonly used to focus the intensity transformation to a particular set of values and progressively attenuating the values that are not in the set. This allows for improving the output of the

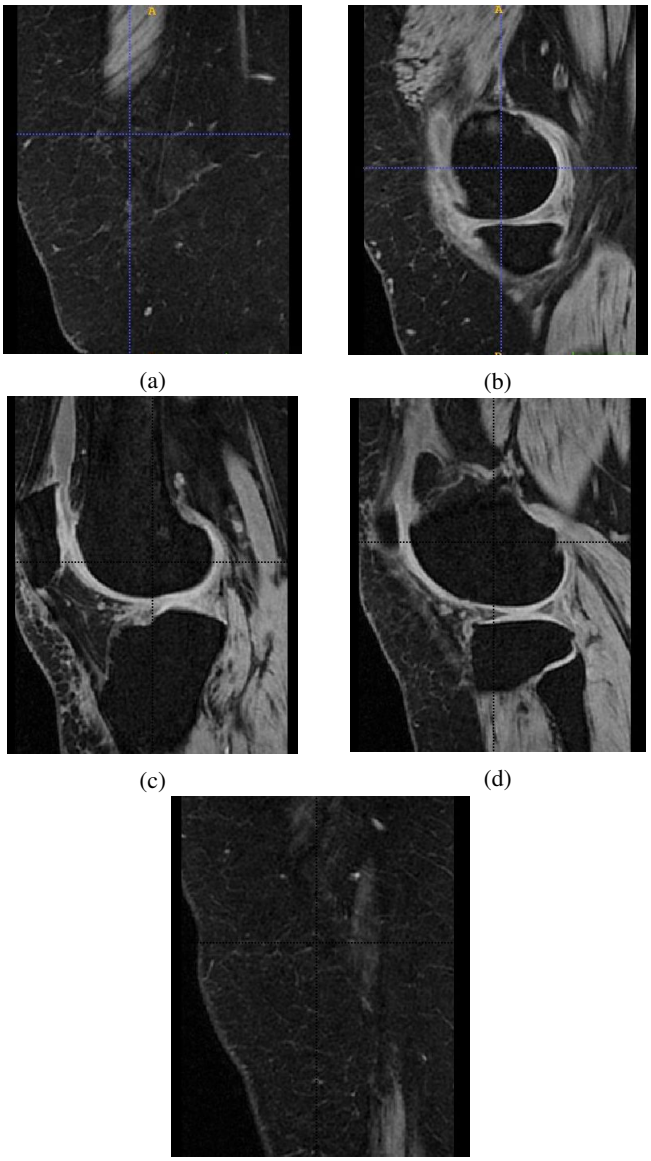

Fig. 5: Division of MRI volume according to anatomical structures.

algorithm as a dedicated edge potential image is input to the geodesic module. Choosing optimal parameters for the sigmoid filter as done carefully in our implementation is of great importance in getting proper segmentation output.

Although the intensities in the bone region vary, there is a reasonable uniform texture throughout the bone region. This gave us an opportunity to supplement the algorithm with edge images based on local variance as proposed in [19]. The results for edge potential images using intensity values and local variance is shown in Fig. 7a and 7b respectively. The edges are represented by dark regions in these images. As one can observe that the image generated using intensities, the bone region is surrounded by a very thin edge layer, but in the variance based image there is a thick layer of edge around the bone. So variance based texture image is a better

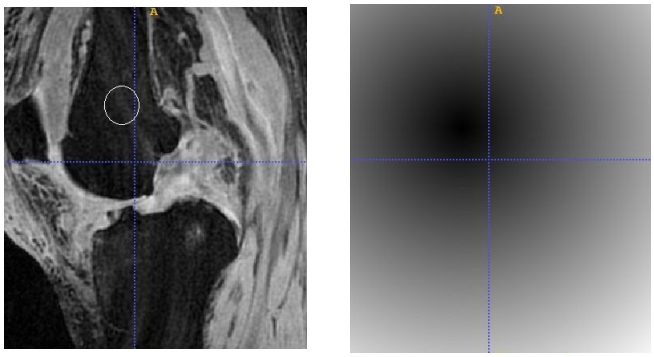

(a) (b)

Fig. 6: Ideal level set (seed) for input to the geodesic contour algorithm.

(a) (b)

Fig. 7: Edge potential images using intensity and variance values.

choice for our application, however both the images were used. The reasons are explained in the following section.

C. Geodesic Active Contour Structures

The input level set of each slice and the corresponding edge potential image are passed through the geodesic active contour filter, originally proposed in [28]. For implementation the *"itk::GeodesicActiveContourLevelSetImageFilter"* block in ITK was used. The intensity and variance based pipelines are treated separately, as also the bone types. Since we are dealing with a 3D volume, it is deemed rational to grow the contour in a 3D space. However, in order to reduce complexity all slices are treated separately.

The curve in the input level set which in our case is a circle grows over the edge image until convergence of an energy function is reached. This is controlled by a propagation term which makes the contour propagate and fit the edges, a curvature term which smoothes the image in areas of high curvature and an advection term which makes the contour adjust better to the boundaries of the object. Optimal parameters for these terms are set using experimentation.

The output for the intensity and variance based geodesic module after binary thresholding is shown in Fig. 8a and 8b respectively. As one can observe, the output based on the intensity values conserves the edge shapes better whereas as

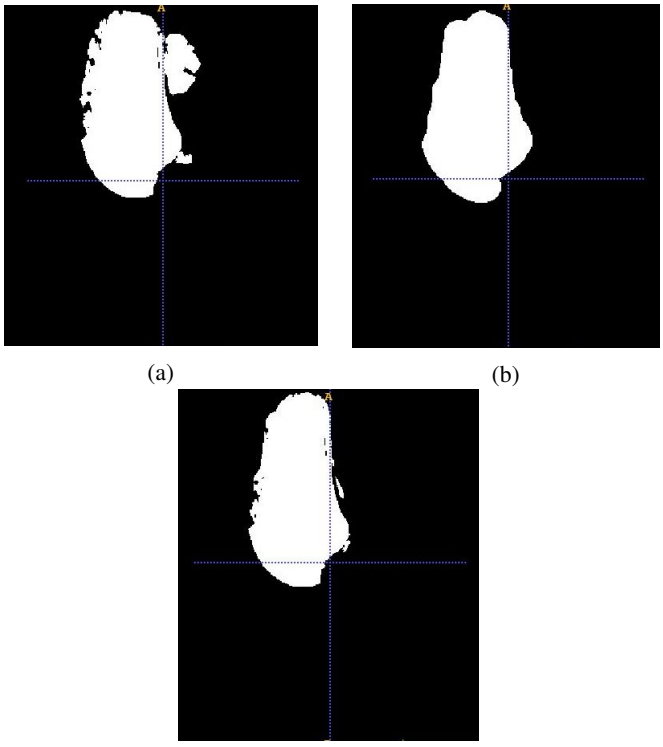

(a) (b) (c)

Fig. 8: Output of the Geodesic Active Contour Shape Modeling based on intensity, variance and the logical operation between the two.

the output based on variance gives smoother regions. So, a logical operation of AND is applied on both images to get the image shown in Fig. 8c. Some small holes are still present in the output which are filled using closing operation.

IV. Cartilage Segmentation

Cartilage is a smooth hyaline spongy material between the tibia and femur bones of knee joint. Articular cartilage covers the patella, tibia and femur in the regions where the bones articulate with one another. The assessment of cartilage dimensions is important for the study of the progression of cartilage damage due to Osteoarthritis (OA) and thereby an accurate segmentation method is desirable in this context.

In this project, femoral and tibial cartilages are obtained by an independent segmentation process. This process starts from analysing the structure and composition of those areas in human knee which reveals that they are highly specialized connective tissues but, unlike most tissues, they do not have blood vessels, nerves, or lymphatics. More specifically, they are composed of a dense extracellular matrix (ECM) with a sparse distribution of highly specialized cells called chondrocytes. The ECM is principally composed of water, collagen, and proteoglycans, with other non-collagenous proteins and glycoproteins present in lower amounts [29]. This suggests the use of a textural information inside these areas in order to distinguish them form their neighboring regions.

A statistical method of examining texture that considers

the spatial relationship of pixels is the color co-occurrence matrix (CCM), also known as the color spatial dependence matrix. A co-occurrence matrix or co-occurrence distribution is a matrix that is defined over an image to be the distribution of co-occurring values at a given offset. The CCM functions characterize the texture of an image by calculating how often pairs of pixels with specific values and in a specified spatial relationship occur in an image, creating a CCM, and then extracting statistical measures from this matrix. There are, in fact, several statistical measures that can be extracted from this matrix. For instance, contrast, energy, correlation, homogeneity, and so on. However, since correlation measure is the joint probability occurrence of the specified pixel pairs, it represents a strong candidate for filtering the cartilage regions in a human knee. Fig. 9 shows an MRI volume for a human knee at the output of a texture filter, in Mevislab, that is based on extracting correlation measure from the CCM matrix.

Inspecting the previous figure shows how both femoral and tibial cartilage regions are marked with higher contrast than the surrounding regions which suggests the use of a region-based segmentation algorithm so as to extract the cartilage from the MRI volume. Region growing algorithm is a good candidate in this context where two blocks of this algorithm were used to segment both femoral and tibial cartilage in a parallel way. The reason why to use two blocks is that the two regions of cartilage are separated from each other and growing in opposite directions. Therefore, forcing the direction of growth of the segmentation algorithm to be consistent with the direction of real growth of these areas will ensure much better results in the 3D volume especially after carefully placing the initial seeds at the regions of interest. Fig. 10 shows the output of both such blocks in Mevislab where the orange regions represent the segmented ones.

The final step is to merge the previously shown results of both cartilage types in one volume. This is, indeed, done by applying some morphological (closing) and logical (AND and XOR) operations in order to obtain the final result which is shown in the Fig. 11.

V. Experimental Results

After obtaining the segmentation results for all four regions separately, the next thing was to combine the regions into one image. First different labels are assigned to each region. Although care has been taken to ensure that no two region overlap each other, still if there are any regions still overlapping they are dealt with by a combination of AND and XOR operations.

The combined regions were next input to the ITK-SNAP software for a qualitative analysis. The segmented output was first overlapped with the ground truth and original MRI images to observe the variations in the output. In few (¡5% on average) of the slices, a higher portion of the output was observed to be misaligned whereas in all the other slices, a very small portion (if any) of the output was observed to be misaligned with the ground truth. 3D model of the knee segmentation was also generated to visually observe the output as shown if Fig. 12. It was observed that the overspreading problem mentioned at the start had been solved and the cartilages were well placed over the bone structures.

In computer vision applications, qualitative analysis is never sufficient because ultimately the output images are used by digital systems. So a quantitative analysis was also carried out. For testing the system, images form the SKI 10 dataset were used. Simultaneously, the quantitative analysis was carried out using the evaluation source code available on their website. The evaluation code give scores to the bone and cartilage regions separately and then takes average of the two to give the final score. The bone score is determined using the average and RMS values of the distance between boundaries of the output and the ground truth whereas the cartilage score is a measure of the overlapping volumes. For both scores, the higher the better. The results for some of the images in the dataset are displayed in tabular form in Table. I.

The average score for bone is 23.7, for cartilage is 32.7 and the overall average score is 28.2. Although it is far from the ideal score of 100, but it is better than some of the published results for SKI 10 challenge. The algorithm took on average around 25 minutes to complete on a standard computer system. The bone score the challenge day image ”Image-091” is zero because of the presence of different type of texture in the bone region. The score would improve if we take input seed contours for each slice separately and let the user adjust parameters according to the input image. However, the main focus of the work was to make the

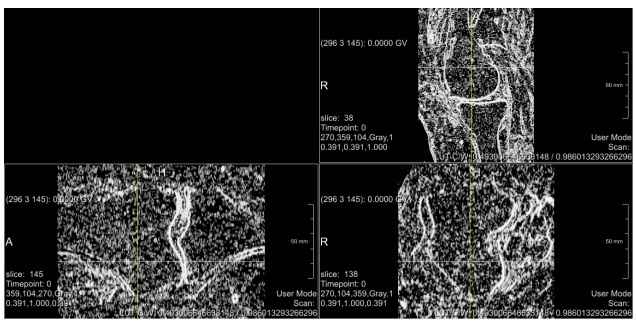

Fig. 9: Textural based filtering for an MRI knee image.

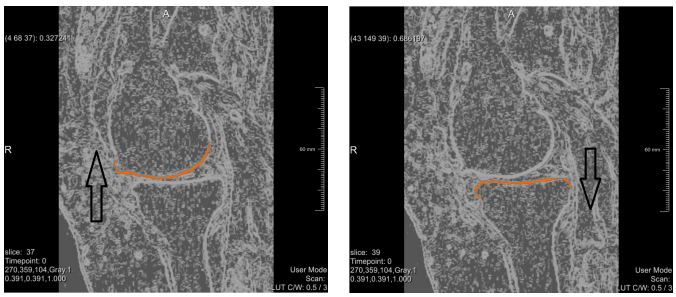

Fig. 10: Output of a region growing algorithm for the filtered volumes.

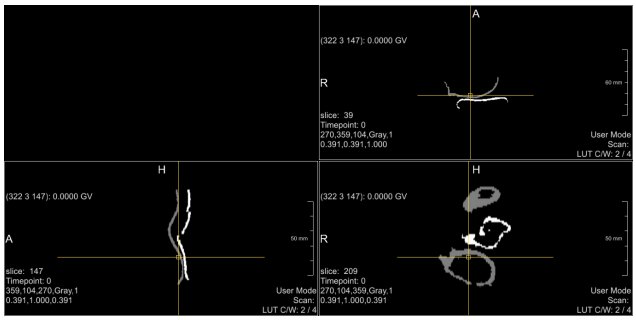

Fig. 11: Final result of segmenting both femoral and tibial cartilage in human knee.

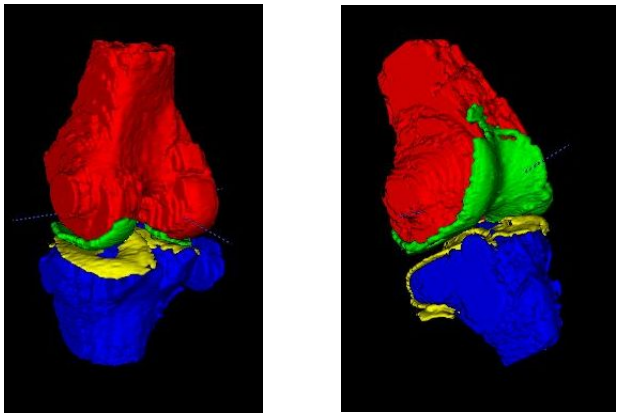

Fig. 12: Rendering of 3D model of the segmentation results using ITK-SNAP.

algorithm as less dependent on user input as possible. So, a trade-off between the accuracy and automation was chosen.

VI. CONCLUSIONS AND FUTURE WORKS

A. Conclusions

This paper presents the work done to segment the femur and tibial regions of the knee joint from MRI images. The bone and cartilage regions were extracted separately. For the bone regions, geodesic active contour structure was implemented on intensity values and local variances whereas for the cartilage regions, region growing was implemented on textured (correlation) version of the input image. The algorithm was successfully tested on SKI 10 dataset with an average score of 28.2. The implementation was done using ITK and Mevislab softwares.

B. Future Works

The analysis revealed few areas that may need to be addressed in future. The 3D model generated had very rough boundaries. This is due to the fact that the algorithm treats every slice separately and then stacks the output of each slices on top of other. The surface quality will improve if the geodesic active contour model is implemented in 3D rather than 2D. Also, currently the intensity and variance models are being treated separately and then combined using logical operators. The two models may be combined together and input as a single model. This will improve results

TABLE I: Results for sample images from the SKI 10 dataset

Image	Bone Score	Cartilage Score	Average Score
Image-061	31.9	39.9	35.9
Image-062	21.0	32.4	26.7
Image-063	28.9	50.6	39.8
Image-064	22.0	25.0	23.5
Image-065	15.7	23.2	19.4
Image-066	21.3	19.7	20.5
Image-067	25.5	24.9	25.2
Image-068	11.0	27.6	19.3
Image-069	39.4	41.4	40.4
Image-083	25.6	16.5	21.0
Image-084	26.1	38.1	32.1
Image-088	38.4	34.7	36.5
Image-072	20.2	62.5	41.4
Image-077	18.4	37.0	27.7
Image-091	0.00	23.4	11.7
Image-100	34.2	25.9	30.1
Average	23.7	32.7	28.2

and decrease run-time. Lastly, since the algorithm is highly dependent on different parameters that have been fined tuned and concealed from the user. These parameters may be further tuned by first classifying the parameters into many classes based on the nature of the input images.

REFERENCES

[1] Shim, H., Chang, S., Tao, C., Wang, J.H., Kwoh, C.K. and Bae, K.T., "Knee Cartilage: Efficient and Reproducible Segmentation on High-Spatial-Resolution MR Images with the Semiautomated Graph-Cut Algorithm Method 1", *Radiology*, vol. 251(2), pp.548-556, 2009.

[2] F. Eckstein, M. Kunz, M. Schutzer, M. Hudelmaier, R. Jackson, J. Yu, C. Eaton, and E. Schneider, Two year longitudinal change and testeretest-precision of knee cartilage morphology in a pilot study for the osteoarthritis initiative, *Osteoarthr. Cartilage*, vol. 15(11), pp. 132632, Nov. 2007.

[3] Sun, Y., E. C. Teo, and Q. H. Zhang, "Discussions of knee joint segmentation." *Biomedical and Pharmaceutical Engineering, 2006. (ICBPE). International Conference on. IEEE*, 2006.

[4] Jiang, Jianguo, Y. Guo, S. Zhan, and H. Li, "Segmentation of knee joints based on improved multiphase Chan-Vese model", *In Bioinformatics and Biomedical Engineering, 2008 (ICBBE) The 2nd International Conference on*, pp. 2418-2422, 2008.

[5] D. L. Pham, C. Xu, and J. L. Prince, Current methods in medical image segmentation, *Annual Review of Biomedical Engineering*, vol. 2, pp. 315-337, 2000.

[6] P. A. Hardya, R. Newmark, Y. M. Liu, D. Meier, S. Norris, D.W. Piraino, and A. Shah, The influence of the resolution and contrast on measuring the articular cartilage volume in magnetic resonance images, *Magn. Reson. Imag.*, vol. 18(8), pp. 965-972, Oct 2000.

[7] C.G. Peterfy et al., Quantification of articular cartilage in the knee with pulsed saturation transfer subtraction and fat-suppressed mr imaging: optimization and validation, *Radiology*, vol. 192(2), 1994.

[8] J. Cibere et al., Reliability of the knee examination in osteoarthritis: effect of standardization, *Arthritis and Rheumatism*, vol. 50(2), 2004.

[9] C. D. Pirnog, "Articular Cartilage Segmentation and Tracking in Sequential MR Images of the Knee", *PhD dissertation, Swiss Federal Institute of Technology Zurich*, 2005.

[10] S. K. Warfield, M. Kaus, F. A. Jolesz, R. Kikinis, "Adaptive, template moderated, spatially varying statistical classification," *Medical Image Analysis*, vol. 4, pp. 43-45, 2000.

[11] S.H. Park, S. Lee, H. Shim, I.D. Yun, S.U. Lee, K.H. Lee, H.S. Kang, and J.K. Han, "Fully automatic 3-D segmentation of knee bone compartments by iterative local branch-and-mincut on MR images from osteoarthritis initiative (OAI)", *Image Processing (ICIP), 2009 16th IEEE International Conference on*, pp. 3381-3384. IEEE, 2009.

[12] V. Lempitsky et al., Image segmentation by branchand-mincut, in *ECCV*, 2008.

[13] V. Grau, A.Mewes, M. Alcaniz, R. Kikinis, and S.Warfield, Improved watershed transform for medical image segmentation using prior information, IEEE Trans. Med. Imag., vol. 23, no. 4, pp. 447458, Apr 2004.

[14] Soh, S. Samson, T.T. Swee, S.S. Ying, C.Z. En, M.N. Mazenan, and L.K. Meng, "Magnetic resonance image segmentation for knee osteoarthritis using active shape models", *In Biomedical Engineering International Conference (BMEiCON), 2014 7th*, pp. 1-5. IEEE, 2014.

[15] J. Folkesson, E. B. Dam, O. F. Olsen, P. C. Pettersen, and C. Christiansen, Segmenting articular cartilage automatically using a voxel classification approach, *IEEE Trans. Med. Imag.*, vol. 26(1), pp. 106115, Jan. 2007.

[16] V. Caselles, F. Catte, T. Coll, and F. Dibos, A geometric model for active contours in image processing, *Numer. Math., 1993*, vol.66 ,pp. 1-31, 1993.

[17] R. Malladi, J. A. Sethian, and B. C. Vemuri, Shape modeling with front propagation: a level set approach, *IEEE Transactions on Pattern Analysis and Machine Intelligence (TPAMI), 1995*, vol.17, pp.158-175, 1995.

[18] C. Xu and J. Prince, Gradient vector flow: a new external force for snakes, *IEEE Computer Society Conference on Computer Vision and Pattern Recognition*, pp.66-71, 1997.

[19] Lorigo, Liana M., Olivier Faugeras, W. Eric L. Grimson, Renaud Keriven, and Ron Kikinis. "Segmentation of bone in clinical knee MRI using texture-based geodesic active contours", *Medical Image Computing and Computer-Assisted Interventation (MICCAI 98)*, pp. 1195-1204. Springer Berlin Heidelberg, 1998.

[20] D. Freedman and T. Zhang, Interactive graph cut based segmentation with shape priors, in *CVPR*, 2005.

[21] M.P. Kumar et al., Obj cut, in *CVPR*, 2005.

[22] Ababneh, Sufyan Y., and Metin N. Gurcan, "An automated content-based segmentation framework: application to MR images of knee for osteoarthritis research", *In Electro/Information Technology (EIT), 2010 IEEE International Conference on*, pp. 1-4, 2010.

[23] Shan, Liang, Cecil Charles, and Marc Niethammer, "Automatic multi-atlas-based cartilage segmentation from knee MR images", *In Biomedical Imaging (ISBI), 2012 9th IEEE International Symposium on*, pp. 1028-1031. IEEE, 2012.

[24] B. Glocker, N. Komodakis, N. Paragios, C. Glaser, G. Tziritas, and N. Navab, Primal/dual linear programming and statistical atlases for cartilage segmentation, *Int. Conf. Medical Image Computing and Computer-Assisted Intervention (MICCAI 2007)*, Brisbane, Australia, Oct. 2007.

[25] T. McInerney and D. Terzopoulos, "Deformable models in medical image analysis: a survey", *Medical Image Analysis*, vol. 1(2) pp. 91-108, 1996.

[26] R. Ronfard, "Region-based strategies for active contour models", *Int'l Journal Comp. Vision*, vol. 13(2) pp. 229-251, 1994.

[27] S. C. Zhu and A. Yuille, "Region competition", *IEEE Trans. Patt. Analysis and Mach. Intell.*, vol. 18(9), 1996.

[28] V. Caselles, R. Kimmel, and G. Sapiro, "Geodesic active contours", *International Journal on Computer Vision*, vol. 22(1), pp. 6197, 1997

[29] J. Sophia, A. Bedi, and A. Redo, "The Basic Science of Articular Cartilage Structure, Composition, and Function", *Sports Health*, vol. 1(6) pp. 461468, Nov 2009